TITLE: Semaphorin 7a promotes breast tumor progression via cell survival, matrix remodeling, and epithelial to mesenchymal transition

AUTHORS: Sarah E Tarullo, Ryan C Hill, Kirk Hansen, Fariba Behbod, Virginia F Borges, Andrew C Nelson, and Traci R Lyons

ABSTRACT: Young women diagnosed with breast cancer (BC) have poor prognosis due to increased rates of metastasis. Additionally, women within 10 years of most recent child-birth at diagnosis are ~3 times more likely to develop metastasis than age and stage matched nulliparous women. We define these cases as postpartum BC (PPBC) and propose that the unique biology of the postpartum mammary gland drives tumor progression. Our published results revealed roles for SEMA7A in breast tumor cell growth, motility, invasion, and tumor associated-lymphangiogenesis, all of which are also increased in pre-clinical models of PPBC. However, whether SEMA7A drives progression in PPBC remains largely unexplored. Our results presented herein show that silencing of SEMA7A decreases tumor growth in postpartum hosts while overexpression increases growth in nulliparous hosts. Further, we show that SEMA7A effects multiple pro-tumor attributes such as cell survival, tumor associated COX-2 expression, fibronectin deposition, and fibroblast-mediated collagen deposition in the tumor microenvironment. Finally, we show that co-expression of SEMA7A/COX-2/FN predicts for poor prognosis in breast and ovarian cancer patient cohorts. These studies suggest SEMA7A as a key mediator of BC progression and that targeting SEMA7A may open avenues for novel therapeutic strategies.

BRIEF SUMMARY: (25 words or fewer)

We identify potential tumor intrinsic and extrinsic roles for SEMA7A in promotion of breast cancer including invasion, modulation of the microenvironment, survival in circulation, and metastasis.

INTRODUCTION: Postpartum breast cancers (PPBC), or breast cancers diagnosed within 5-10 years of last childbirth, are nearly three times as likely to become metastatic and result in death from breast cancer(1-3). Specifically, PPBC patients diagnosed within five years of last competed pregnancy exhibit distant metastasis free five-year survival (DMFS) rates as low as 70%(1), which are further decreased to 50% after ten years(2). Using this definition, PPBC may account over half of breast cancers diagnosed in women aged <45 (1). Using a pre-clinical model of PPBC we have shown that pre-invasive, non-metastatic breast cancer cells, MCF10DCIS, become invasive and metastatic if they are implanted into mouse mammary tissues during the normal physiological process of postpartum mammary gland involution(4). The MCF10DCIS model closely resembles ductal carcinoma in situ (DCIS) and progresses to invasive ductal carcinoma (IDC) similar to what is seen in some breast cancer patients(5). This model allows for monitoring early events in the metastatic cascade, such as the transition from in situ to invasive disease, and xenograft studies have revealed that postpartum/post-lactational changes to the mammary tissue microenvironment promote invasion and metastasis in this model(4, 6, 7).

Postpartum/post-lactational mammary involution is a tissue-remodeling event that returns the gland to the pre-pregnant state after childbirth and/or lactation. We and others have shown that programs associated with mammary gland involution are similar to wound healing and tumor-promotional microenvironments(1, 4, 6, 8-16), which led us to investigate whether the tissue microenvironment created during postpartum involution contributes to tumorigenesis and progression. Previously, we published a preclinical triple negative breast cancer model of PPBC where MCF10DCIS xenografts in recently-weaned, or postpartum, mice exhibit accelerated growth and progress from *in situ* to invasive disease at more rapidly when compared to those injected into nulliparous hosts(4). This progression is driven, in part, by collagen deposition and collagen mediated expression of COX-2, which promotes tumor cell invasion. Recently, we have shown that Semaphorin 7a (SEMA7A) expression is increased in mouse and human mammary tissues after pregnancy, in the mouse mammary epithelium during the tissue remodeling phase of involution, and in tumors that outgrew after orthotopic implantation during postpartum involution(9). Furthermore, we observed that overexpression of SEMA7A in mouse mammary tumor cells accelerates tumor growth in nulliparous hosts to the same level observed in postpartum hosts. Additionally, MCF10DCIS cells stably transfected with shRNAs designed to silence SEMA7A in human derived breast cancer cell lines exhibit decreased in vivo growth and invasion in nulliparous hosts(17). Finally, SEMA7A gene expression is increased in breast cancer datasets where expression associates with decreased overall survival(17).

Semaphorins are proteins characterized for their roles in axon guidance and immune-modulation, however, others have also reported roles for semaphorins multiple cancer types(18, 19). Furthermore, SEMA7A expression, either alone or in combination with expression of other known pro-tumorigenic molecules, is emerging as poor prognostic indicator for multiple tumor types including breast, lung, and melanoma(9, 17, 20-24). Here, we show that SEMA7A protein is expressed in DCIS from breast cancer patients, is necessary for postpartum tumor progression in our pre-clinical model, and sufficient to drive tumor progression in non-postpartum hosts. We also demonstrate a connection between collagen, COX-2, and SEMA7A. Specifically, we show that SEMA7A is sufficient to drive collagen deposition in the tumor microenvironment (TME) via upregulation of collagen I mRNA expression by fibroblasts, which results in tumor cell expression of COX-2 and invasion. Furthermore, we propose a pro-survival role for SEMA7A through alterations in the ECM that is mediated through the downstream activation/phosphorylation of AKT. Finally, we identify SEMA7A dependent expression of another extracellular matrix protein, fibronectin (FN), which is also a characteristic of cells that have undergone EMT. To establish whether this mechanism is at play in aggressive breast cancers, we demonstrate that a gene signature of SEMA7A, PTGS2 (encodes for COX-2), and FN1 results in significantly decreased distant metastasis free survival in breast cancer patients compared to FN alone, which is a known mediator of poor prognosis. Taken together, our results suggest that SEMA7A plays a role in progression of PPBC through activation of pro-invasive and pro-survival programs in breast cancer, which merits further studies to develop a novel therapeutic for breast cancer patients.

RESULTS

SEMA7A protein is highest in DCIS from PPBC patients and promotes tumor growth via activation of cell survival mechanisms

To investigate expression levels of SEMA7A protein in normal breast tissue and DCIS from patients we performed immunohistochemistry (IHC) on a tissue array consisting of surgical specimens from normal

adjacent breast and ductal carcinoma *in situ* (DCIS) lesions from the same patient in addition to DCIS lesions from women in our University of Colorado Young Women's breast cancer cohort (Figure 1A). Samples from kidney and placenta were included in the array as negative and positive controls, respectively (SFigure 1). We observed that expression levels of SEMA7A were significantly increased in the DCIS compared to normal breast tissue (Figure 1B). Additionally, overall SEMA7A expression in DCIS from our young women's breast cancer (YWBC) cohort was similar (Figure 1A). To determine whether postpartum patients exhibit higher SEMA7A expression, we separated the DCIS from our young cohort by never pregnant (nulliparous) and within 5 years of most recent childbirth (postpartum) and observed ~40% average positivity for SEMA7A in the postpartum group versus ~30% in nulliparous (Figure 1B). These results suggest that, amongst our young patients, SEMA7A is highest on average in DCIS in postpartum women where it may be involved in DCIS progression.

To examine whether SEMA7A drives tumor growth in our established pre-clinical model of postpartum DCIS progression, we orthotopically injected MCF10DCIS cell lines that stably express a SEMA7A targeted shRNA (shSEMA7A) or nontargeting control (Crtl)(17) at involution day 1 (Figure 2A, inset Figure 2B). We observed that silencing of SEMA7A is sufficient to decrease tumor growth in postpartum hosts (Figure 2B & STable 1). Of note, due to the absence of selective pressure in vivo, some tumor cells regained expression of SEMA7A and started to grow, however, at study end, expression of SEMA7A in the knockdown group remained significantly lower than the control group (SFigure 2A). To determine whether SEMA7A expression alone is sufficient to drive DCIS progression in nulliparous hosts, we injected MCF10DCIS cells engineered to express ~4-fold higher SEMA7A protein (SEMA7A OE), along with vector only controls (inset Figure 2C), and observed that SEMA7A overexpressing tumors exhibited increased/accelerated growth (Figure 2C). Since it is widely recognized that tumor growth is driven by activation of pro-proliferative and/or pro-survival pathways, and we have previously shown that postpartum tumors and SEMA7A expressing tumors are more proliferative in independent studies (4, 17), we examined Ctrl and shSEMA7A tumors for a proliferation marker (Ki67). Surprisingly, we did not see any significant changes in Ki67 (Figure S2B). We then examined cleaved caspase 3, a marker of apoptosis, and observed an increase in shSEMA7A tumors and a corresponding decrease with overexpression suggesting that SEMA7A promotes cell survival (SFigure 2C&D). One known mechanism of cell survival co-opted by tumors cells is activation of pro-survival kinase AKT. Thus, we measured levels of activated AKT via immunoblot for pS473 and observed decreased levels in shSEMA7A tumors and increased levels in SEMA7A OE (Figure 2D, SFigure 2E). We then measured cell death by examining cleaved caspase 3/7 in our shSEMA7A and SEMA7A OE cells in vitro to reveal increased death with shSEMA7A and decreased with SEMA7A OE in the MCF10DCIS cell lines. We further validated this finding in an additional triple negative breast cancer cell line, MDA231 (Figure 2G&H). We also measured cell growth and death in real time to confirm that silencing of SEMA7A increases cleaved caspase-3/7 (SFigure 2F). Thus, we suggest that SEMA7A promotes tumor growth via activation of pro-survival signaling mediated by AKT.

SEMA7A drives collagen mediated expression of COX-2 to promote tumor cell invasion

To examine whether SEMA7A drives progression of in situ to invasive lesions (IDC) over a time course in our postpartum model, tumors were scored for invasion. The time course of DCIS progression to invasive is summarized in SFigure 3. In our postpartum model tumors were scored for invasion at 5 weeks revealing that 87% of the tumors in the control group were IDC compared to only 33% of the shSEMA7A (KD). Further, only 12.5% of the control tumors were IDC+DCIS compared to 56% of the tumors in the shSEMA7A group. Finally, while none of the control tumors were maintained in a non-invasive state, 11% of tumors in the shSEMA7A group were DCIS with evidence of microinvasion (Figure 3A). Next, we tested whether SEMA7A OE tumors in a nulliparous mice exhibit accelerated invasion by examining tumors at 3 weeks post injection. As expected,

control tumors were all DCIS; however, greater than 50% of the tumors from the SEMA7A OE cells had DCIS+microinvasion and/or were IDC+DCIS (Figure 3B). These results suggest that SEMA7A accelerates invasive progression in postpartum hosts and is sufficient to initiate invasion in nulliparous hosts.

Collagen mediated upregulation of COX-2 is a dominant feature of tumor cell invasion in our postpartum model(4). Therefore, we quantitated COX-2 staining in our SEMA7A knock down and over-expression models to determine if COX-2 levels were consistent with the observed reduction or promotion of invasion, respectively. We observe that COX-2 expression was significantly decreased in the postpartum shSEMA7A tumors (Figure 3C). Likewise, we observed consistently upregulated COX-2 in our SEMA7A OE tumors versus controls in nulliparous hosts (Figure 3D). To determine if the observed increase in COX-2 was mediated by collagen, we quantified fibrillar collagen (blue) in our postpartum shSEMA7A and nulliparous SEMA7A OE tumors to show that alterations in SEMA7A expression correlate with overall collagen content (Figure 3E&F). Finally, to determine if SEMA7A drives invasion independent of collagen and COX-2, we measured invasion in a 3D organoid model with SEMA7A OE cells suspended in matrigel. We found that SEMA7A overexpression alone was insufficient to drive increased invasion (Figure 3G). However, with the addition of collagen to matrix, overexpression of SEMA7A was sufficient to increase the incidence of invasive organoids (Figure 3H). We further confirmed this relationship using the MDA231 model to demonstrate that knockdown of SEMA7A was sufficient to decrease the incidence of invasive organoids on collagen (Figure 3I).

Since fibroblasts are the main producers of collagen in the TME, we utilized a general fibroblast marker, αSMA, to examine whether SEMA7A dependent fibroblast infiltration occurs in our tumors but observed no differences (SFigure 4A). To determine whether postpartum tumors differentially signal to fibroblasts via shedding of SEMA7A from the tumor cell, we measured SEMA7A in conditioned medias from postpartum and nulliparous tumor cell populations ex vivo. Our results show that postpartum tumor cell populations shed more SEMA7A on average than nulliparous (Figure 4A). Then, we treated cultured fibroblasts with conditioned media from our SEMA7A overexpressing tumor cells and controls, to reveal that conditioned medias from SEMA7A overexpressing cells induce *COL1A1* gene expression in fibroblasts (Figure 4B). Finally, to show that SEMA7A specifically drives increased *COL1A1* expression we treated fibroblasts with purified SEMA7A which also resulted in a significant increase in COL1A1 expression (Figure 4C). Hence, while SEMA7A does not appear to increase fibroblast migration/infiltration into tumors, our results suggest SEMA7A as an important mediator of tumor cell invasion by influencing collagen deposition into the TME by fibroblasts.

SEMA7A drives mesenchymal cell phenotypes

To understand additional SEMA7A mediated changes to the TME we performed an unbiased mass spectrometry analysis of tumor conditioned medias from tumors ex vivo that were derived from shSEMA7A or control cells. When we specifically examined peptides collected from secreted proteins of human origin, we observed striking changes in fibronectin (FN), which was significantly decreased with the silencing of SEMA7A (Figure 5A). We then confirmed decreased expression by quantifying FN protein expression in our shSEMA7A, SEMA7A OE tumors and respective controls (Figure 5B). As FN is frequently associated with epithelial-to-mesenchymal transition (EMT) and provides a template for collagen fibrillogenesis, we tested if SEMA7A expression also promotes mesenchymal phenotypes to promote cell invasion. We measured cellular morphology, by measuring cell aspect ratios with the prediction that ratios >1 would be indicative of mesenchymal-like cells since their elongated phenotype renders their length greater than their width, and that epithelial-like cells, which are more cuboidal, would have a ratio of ~1(25). Our results reveal that shSEMA7A

MDA-231 cells exhibit decreased average aspect ratios from 8 to 3(Figure 5C). Furthermore, SEMA7A OE in the MCD10DCIS model was sufficient to increase the average aspect ratio from 1 to 3 (Figure 5D). To extend our observations, we also observed additional markers associated with mesenchymal and invasive phenotypes in our ex vivo mass spectrometry analysis including members of the S100 family of proteins, matrix metalloproteinase-2 (MMP2), and vimentin (Figure 5E-L) to show downregulation. These results suggest that SEMA7A promotes expression of mesenchymal-associated proteins.

SEMA7A drives cell survival and metastatic potential via FN

Interestingly, FN signals via integrins, which are upstream of pro-survival pathways, such as AKT. Thus, we hypothesized that the increase in cell death observed in shSEMA7A silenced cells was due to their inability to produce FN and activate pro-survival signaling. To determine if FN could rescue cell death, we plated shSEMA7A cells on FN, with laminin and collagen as controls. Surprisingly, increased cell death occurred on laminin and collagen, but not on FN, which resulted in levels of cell death that were similar that of Ctrl cells (Figure 6A). These results suggest that exogenous FN can rescue cell death in the shSEMA7A cells, which cannot make their own FN. Thus, we suggest that SEMA7A promotes cell survival along the metastatic cascade by providing tumor cells with FN independent of their microenvironment.

The first steps in the metastatic cascade involves cell detachment from ECM to facilitate invasion and access to the vasculature via intravasation; next, cells must survive matrix detached conditions in circulation (anoikis resistance) and finally extravasation must occur, which is required for seeding of metastatic sites. To assess a role for SEMA7A in promoting survival in circulation, we forced cellular detachment in culture and performed anokis resistance assays. Similar to our results with attached cells, we observe that SEMA7A promotes cell survival in detached conditions in both MCF10DCIS and MDA231 cells as measured by cleaved caspase-3/7 activity (Figure 6B&C). To assess whether SEMA7A promotes anoikis resistance and outgrowth of distant metastasis in vivo, we performed tail vein injections of MDA231 shSEMA7A or Ctrl and assessed for pulmonary metastasis. Our results show an increase in number of metastatic lesions per lung as well as increased average size of the lung metastasis (Figure 6D). These results suggest that SEMA7A plays a role survival, seeding, and outgrowth during the metastatic cascade.

SEMA7A, COX-2, FN signature correlates with increased metastasis in breast cancer patients

In the METABRIC and KmPlot datatsets SEMA7A expression decreases overall survival (OS) (17) (SFigure 6A); however, SEMA7A expression alone does not significantly associate with decreased distant metastasis free survival (DMFS) (SFigure 6B). Additionally, although transcripts for COX-2, SEMA7A, and FN are all upregulated in breast cancer compared to normal tissue (SFigureC), only decreased FN gene expression is associated with significantly decreased DMFS, HR=1.3 (95% CI: 1.07-1.58, p=0.0032) (SFigure 6D-E). However, when co-expression of COX-2, SEMA7A, and FN1 were examined by Kaplan-Meyer analysis for DMFS of all breast cancers we observed that high expression of all three genes significantly increased risk for metastasis HR=1.9 (95% CI: 1.31-2.74, p=0.00052) with 5 year DMFS rates approaching 70%, which is similar to what we have observed in our postpartum patients(1) (Figure 6E). Further, SEMA7A expression significantly correlated with both FN and COX-2 in all breast cancers, suggesting our observations in postpartum breast cancer may be relevant to all breast cancer cases expressing this signature (Figure 6F&G). Finally, we observe a similar relationship with our three gene signature and progression free survival in ovarian tumor datasets suggesting that our observations have implications beyond breast cancer (Figure 6H).

DISCUSSION

Postpartum breast cancer patients diagnosed within five years of most recent childbirth have been described as a high risk population for relapse and metastasis and comprise nearly 30% of all breast cancers diagnosed in women aged <40 in both US and Norwegian cohorts(1). Recent results extend the risk for metastasis to 10 years postpartum, which makes the percentage of young breast cancer patients who are considered postpartum and as such at high risk for metastasis nearly 50%(26). A recent publication by Welch and Hurst defines the hallmarks of metastasis as motility and invasion, modulation of the microenvironment, plasticity and colonization(27). Here, using pre-clinical models, we identify potential tumor intrinsic and extrinsic roles for SEMA7A in promotion of PPBC growth including invasion, modulation of the microenvironment, survival in hostile environments such as the circulation, and colonization. Our results suggest that SEMA7A mediated tumor cell survival occurs via an intrinsic mechanism that involves downstream activation of pro-survival kinase AKT, but also through fibronectin secretion into the tumor microenvironment. Further, we show that shed SEMA7A increases collagen deposition via fibroblasts in the TME. In turn, collagen increases tumor cell expression of COX-2 expression, which drives invasion. We also show that SEMA7A supports tumor cell invasion by inducing mesenchymal phenotypes. Finally, we show that SEMA7A promotes anoikis resistance and colonization of distant organs. Thus, we suggest that SEMA7A plays a key role in the development of metastatic disease. We further support this claim with a three-gene signature consisting of COX-2, SEMA7A, and FN that not only correlates with distant metastasis formation in breast cancer patients, but also decreases progression free survival in patients with ovarian carcinoma as well. We propose a model in which SEMA7A signaling may support multiple aspects of metastatic progression in PPBC and in breast cancer in general (Figure 7).

SEMA7A was first recognized for its expression on lymphocytes and was designated CD108w(28). Subsequently, CD108w was termed SEMA7A due to its structural similarities with members of the Semaphorin family of proteins. Structurally, SEMA7A is unique in the semaphorin family as it is the only semaphorin linked to the membrane via a glyocosylphospahtidl-inositol (GPI) anchor and that signals to β1-integrin(29). The GPI anchor of SEMA7A can be cleaved to result in shedding of SEMA7A into the extracellular environment, which promotes β1-integrin dependent mechanisms of inflammation and fibrosis(30-35). In fibrosis, TGFβ induces SEMA7A and β1 integrin expression, which activates AKT signaling to result in upregulation of extracellular matrix (ECM) molecules such as collagen and fibronectin to promote formation of fibrotic lesions(36). Furthermore, in cancer, SEMA7A-β1-integrin binding promotes tumor growth, tumor cell epithelial to mesenchymal transition (EMT), migration, invasion, metastasis, and neo-vasculogenesis(20-22). Our results showing that SEMA7A promotes similar pro-survival mechanisms in models of triple negative postpartum breast cancer may provide both mechanistic and clinical insight into why postpartum patients and/or triple negative breast cancer patients with high expression of SEMA7A, exhibit poor survival rates. Although not directly addressed herein, we hypothesize that SEMA7A turns on AKT signaling via both direct binding to β1-integrin and secretion of FN, which have both been shown to activate PI3K/AKT(37-39) signaling. Of particular note, AKT can activate NFκB(40-43), a transcription factor that can upregulate both COX-2 and SEMA7A expression(44, 45). Given that silencing of COX-2 results in decreased SEMA7A expression(17), we suggest that AKT activation of NFκB may function in a feed-forward loop to COX-2 mediated expression of SEMA7A, cell survival and invasion (Figure 7).

We also suggest that FN may act downstream of SEMA7A to promote mesenchymal phenotypes and tumor cell invasion. Since previous studies have shown that FN engagement of $\alpha_v\beta_1$ integrin activates the transcription factor Slug, which is known to promote transcription of mesenchymal genes EMT(46, 47). Interestingly, SEMA7A has been directly linked to EMT where the authors show that TGFβ is unable to induce an EMT without SEMA7A(20). Additional studies aimed at better understanding of how SEMA7A contributes to EMT are necessary to understand the role of this mechanism in PPBC

We further demonstrate that SEMA7A is involved in an additional, but not unrelated, signaling axis that may alter the tumor microenvironment through fibroblast mediated production of collagen. Our previous results have shown that collagen deposition occurs during postpartum mammary gland involution(4) and fibroblasts are uniquely activated during postpartum involution to display pro-tumorigenic activity(13). In addition, a single pregnancy is sufficient to convert the high collagen content of the postpartum breast into pro-tumorigenic collagen(48). Finally, it has long been recognized that increased breast density, primarily driven by collagen, increases risk for developing breast cancer(49, 50). Thus, our results suggest that SEMA7A expression on the mammary epithelium during involution may promote the increased collagen deposition observed, which may play a role for the increased risk for developing breast cancer that can be attributed to recent pregnancy (1, 4, 7, 26, 50-52).

Given that SEMA7A, COX2, and FN are associated with an increased risk for metastasis in breast cancers regardless of subtype or treatment regimen. It is also possible that SEMA7A may promote resistance to current therapies for breast cancer. For example, it has been shown that SEMA7A promotes resistance to EGFR targeted therapies in lung cancer(53). Interestingly, it has shown that estrogen and/or progesterone promote SEMA7A expression in the hypothalamus, suggesting that hormone signaling may promote elevated levels of SEMA7A in breast cancers(54). Consistent with this hypothesis another member of the semaphorin family, Semaphorin 4C, promotes breast cancer growth, invasion, and in hormone driven cancers, hormonal independence(55). Additionally, both AKT and FN have been shown to promote tamoxifen resistance(56-63). Thus, since estrogen receptor positive patients comprise the largest percentage of breast cancer patients, perhaps SEMA7A signaling drives estrogen receptor positive patients to not respond favorably to anti-estrogen based therapies. Furthermore, AKT signaling has been shown promote additional mechanisms of drug resistance to chemotherapeutics via activation of pro-survival and anti-apoptotic signaling(64-67) and decreased sensitivity to tyrosine kinase inhibitors has also been associated with upregulation of EMT markers and pathways(20, 68-71) . Finally, EMT induced transcription factors such as Snail, Slug, and Zeb1 regulate additional pro-survival mechanisms, which result in resistance to chemotherapeutic treatments(72-79). Future studies are needed to better understand how the complex interplay between SEMA7A, hormones, and subsequent downstream signaling may contribute to cancer progression and treatment resistance. Importantly, we show for the first time that SEMA7A protein is expressed at increased levels in patient samples of DCIS, compared to normal tissues, and we have identified SEMA7A as a key mediator of PPBC invasion in our pre-clinical model. Currently, there are no targeted therapies or specific treatment options for women diagnosed with PPBC. Furthermore, there are no clinical parameters for predicting whether DCIS will progress to invasive disease. We propose that targeting SEMA7A could be a predictive biomarker for disease progression as well as a potential therapeutic option for women with breast cancer. If direct targeting of SEMA7A is not feasible, SEMA7A activates many downstream targets such as FAK, Src, and ERK(24, 80, 81), for which targeted therapies are in various stages of development and clinical trials.

Although current and past clinical trials in breast cancer for some of these targeted inhibitors have been unsuccessful, perhaps SEMA7A could serve as a biomarker for patients who have hyper-activation of these pathways and thus benefit from targeted therapies.

MATERIALS AND METHODS

Cell Culture and reagents

MCF10DCIS.com cells were obtained from K. Polyak and A. Marusyk (Harvard University, Cambridge, MA). MDA-231 cells were obtained from P. Schedin (Oregon Heath and Sciences University, Portland OR). HLF-1 cells were gifted from M. Fini (University of Colorado Anschutz Medical Campus, Denver, CO). Cells were validated by the DNA sequencing core at the University of Colorado Anschutz Medical campus and identified to be a pure population of their respective cell lines. Cells were regularly tested for mycoplasma throughout studies. Cells were sub-cultured as previously described, or according to ATCC standards(4, 82). shRNA silencing was achieved using shRNA SEMA7A targeting plasmids (SABiosciences, Frederik, MD, and Functional Genomics Facility at University of Colorado Anschutz Medical Campus, Denver, CO) and confirmed via qPCR and Western blot analysis. Overexpression plasmid (SEMA7A-Fc) was a generous gift from R. Medzhitov (Yale University, New Haven, CT). Control plasmid (pcDNA3.1) was obtained from H. Ford (University of Colorado Anschutz Medical Campus, Denver, CO). All other overexpression plasmids (p304-V5-Blasticidin and V5-SEMA7A) were obtained from the Functional Genomics Core at the University of Colorado Anschutz Medical Campus and confirmed via qPCR and Western blot analysis. Purified SEMA7A was isolated from MDA-231 cells engineered to overexpress SEMA7A-Fc in collaboration with the Protein Purification/MoAB/Tissue culture core at the University of Colorado Anschutz Medical Campus. 3D cultures were performed as previously described (4, 17).

RNA isolation

RNA was isolated using the Quick-RNA kit (Zymo Research Irvine, CA,). Concentration and purity were assessed using absorbance at 280 nm, 260 nm, and 230 nm. cDNA was synthesized from 1 ug RNA using the Bio-Rad (Hercules, CA) iScript cDNA Synthesis Kit in the following conditions: 25ºC for 5 min, 42ºC for 30 min, and 85ºC for 5 min.

qPCR analysis

qPCR of cDNA samples was performed using the Bio-Rad iTaq Universal SYBR Green Supermix with primers for *SEMA7A, COL1A1, COX-2* (Bio-Rad PrimePCR, Hercules, CA) and *FN1* (forward: GCCAGTCCTACAACCAGTATTC , reverse: CTAAGCTGGGTCTGCTAACATC) The conditions were as follows: 95ºC for 3 min, then 40 cycles of 95ºC for 15 sec and 60ºC for 1 min, 95ºC for 30 sec and 55ºC for 1 min. The fidelity of our primers was assessed after each qPCR experiment using a 95ºC melt curve. mRNA quantification was normalized using the geometric average of two reference genes, *GAPDH* (forward: CAAGAGCACAAGAGGAA GAGAG, reverse: CTACATGGCAACTGTGAGGAG) and *RPS18* (forward: GCGAGTACTCAACACCAACA, reverse: GCTAGGACCTGGCTGTATTT).

Western blot analysis

Western blots were performed by loading equal amounts of protein into each lane. Protein concentration in lysates was determined by Bradford assay. SEMA7A blots were probed with anti-SEMA7A (clone:C6-Santa Cruz Biotechnologies, Dallas, TX) and goat anti-mouse secondary (Abcam, Cambridge, MA). Blots were then exposed and developed on film. Phosho-AKT(S473) blots were probed with phospho-specific and total antibodies (Cell Signaling Technologies, Danvers, MA) and donkey anti-mouse or anti-rabbit (LiCOR, Lincoln, NE, USA). Blots were imaged and quantitated on an Odyssey CLx Imager (LiCOR).

Animal model

The postpartum model was used as previously described (4). Briefly, 6-8 week old female SCID Hairless Outbread mice from Charles River were bred and after birth, pups numbers were normalized to 6-8 pups per dam, after 10-13 days of lactation, pups were removed to initiate involution (Day 0). Then, 250K MCF10DCIS.com controls and cells with shSEMA7A were injected the next day (involution day 1) into the left and right #4 mammary fat pads. For SEMA7A overexpressing studies 6-8 week old Nude athymic (nulliparous) mice from Charles river were similarly injected. Tumors were measured using calipers twice weekly and volumes calculated based on the length, width, and height of the tumor (volume of a sphere). For metastasis studies, nude mice were injected with $1x10^6$ cells into the tail vein. Animals were monitored for weight loss and sacrificed 40 days post injection.

Histologic analysis

Tumors were harvested at 5 weeks (shSEMA7A studies) or 3 weeks (SEMA7A overexpression studies). Mammary glands with intact tumor were prepared for immunohistochemistry as previously described (cite). Hematoxylin and eosin stained sections of tumors were examined by a board-certified anatomic pathologist (ACN) who was blinded to experimental group. Tumors were scored for invasive as follows: 0-lesions which contained only well-devolved DCIS structures with clearly defined basement membranes and no evidence of microinvasion; 1-lesions that contained extensive DCIS with identifiable micro-invasive foci; 2-lesions that contained significant areas of sheet-like invasive tumor growth and mixed with areas of DCIS; 3-lesions that contained entirely invasive tumor with rare to absent DCIS remnants. Human breast tissue (normal and DCIS) samples were obtained from a collaboration with F. Behbod at the University of Kansas Medical Center. The Young Women’s Breast Cancer Cohort and subsequent nulliparous and postpartum cases were identified through our young women’s breast cancer database and tissue collection, which was created under a Colorado Multiple Institution Review Board–approved and subject consent–exempt protocol.

Immunohistochemistry and Immunofluorescence

Antibody information is provided in Supplementary Table 2. For FN and COX-2 400X images were taken of intact tumor and quantitated using ImageJ software. For SEMA7A, cleaved caspase-3, and trichrome stain quantification of total tumor area (necrotic and stromal areas removed) and percent positive stain or stain intensity was performed using Image Aperio Analysis software (Leica, Buffalo Grove, IL). Areas for quantification were annotated using Aperio analysis tools and percent weak, medium, and strong determined using the color-deconvolution tool. Immunofluorescent images were obtained using 400X magnification on OLYMPUS microscope.

Analysis of publicly available datasets

Km plotter was used to determine distant metastasis free survival and levels of expression of mRNA in normal versus breast cancer(83). Briefly, in Km plot for breast cancer or ovarian cancer, SEMA7A, PTGS2 (COX-2), and FN1 were queried using the multigene classifier using the mean centered option for distant metastasis free survival (DMFS) or progression free survival (PFS), respectively. Kaplan-Meier plotter is capable of assessing the effect of 54,675 genes on survival using 10,461 cancer samples. This includes 5,143 breast cancer samples with a mean follow-up of 69 months. Ovarian cancer samples include both endometrial and serous subtypes. CBioPortal analysis was conducted using the Breast Invasive Carcinoma (TCGA provisional) dataset, RNA seq V2, with a z score of +/- 1.0.

Mass spectrometry analysis

Small tumor pieces (~1mm) were placed on gelatin sponges (Novartis Animal Heath, Greensboro, NC, USA) in serum free media. After 48 hours tumor conditioned media was collected and spun down to remove any cellular debris. Equal volume media samples representing ~ 30 µg of total protein were directly loaded onto a pre-washed 10 kD molecular weight cut-off filter and digested utilizing the filter aided sample digestion (FASP) protocol as previously described(84). Briefly, samples were reduced, alkylated, and enzymatically digested with trypsin. Resulting peptides were concentrated and de-salted by solid phase extraction utilizing in-house made stage tips made with Sytrene Divinyl Benzene disks (Empore™). Liquid chromatography tandem mass spectrometry (LC-MS/MS) was performed on a Thermo nanoEasy LC II coupled to a Q Exactive HF. MS acquisition parameters are detailed previously(85). Raw files were searched with Proteome Discoverer 2.2 against the *Mus Musculus, Homo Sapiens, and Bos Taurus* uniprotKB database in Mascot. Precursor mass tolerance was set to +/- 10 ppm and MS/MS fragment ion tolerance of +/- 25 ppm. Trypsin specificity was selected allowing for 1 missed cleavage. Variable modifications include Met oxidation, proline hydroxylation, protein N-terminal acetylation, peptide N-terminal pyroglutamic acid formation, and a fixed modification of Cys carbamidomethylation. Search results were visualized using Metaboanalyst v4.0(86) and gene ontology mapping was done using PANTHER(87).

Statistical Analyses.

Unpaired t-tests, ANOVA, and Kaplan Meyer analysis were performed in GraphPad Prism, assuming independent samples and normal distributions. All analyses were done using two-tailed p-value, except for Figure 1C, where one-tailed analysis was used.

Acknowledgements

We gratefully acknowledge K. Polyak and A. Maruskyk for providing MCF10DCIS parental cells; P. Schedin for providing MDA 231 parental cells; M. Fini for the HLF-1 fibroblast cells; H. Ford for the pcDNA3.1 vector; and R. Medzhitov for the SEMA7A-Fc overexpression vector. We also acknowledge V. Wessells, A. Elder, L. Crump, T. Wallace, C. Young, and C. Hoang for technical support and advice. This work was supported by the American Cancer Society (RSG 16-171-01-CSM), and NIH/NCI (R01CA211696-01A1 to T. Lyons; NIH/CCTSI/CTSA (TL1 TR001081) to S. Tarullo.

References

1. Callihan EB, Gao D, Jindal S, Lyons TR, Manthey E, Edgerton S, et al. Postpartum diagnosis demonstrates a high risk for metastasis and merits an expanded definition of pregnancy-associated breast cancer. *Breast cancer research and treatment.* 2013;138(2):549-59.

2. Erica T. Goddard SB, Troy Schedin, Sonali Jindal, Jeremy Johnston, Ethan Cabral, Traci R. Lyons, Motomi Mori, Pepper J. Schedin, Virginia F. Borges. Defining the impact of a postpartum diagnosis on metastasis and the clinical features underlying risk: A young women's breast cancer cohort study. *Jama Network.* 2018;In press.

3. Nichols HB, Schoemaker MJ, Cai J, Xu J, Wright LB, Brook MN, et al. Breast Cancer Risk After Recent Childbirth: A Pooled Analysis of 15 Prospective Studies. *Ann Intern Med.* 2018.

4. Lyons TR, O'Brien J, Borges VF, Conklin MW, Keely PJ, Eliceiri KW, et al. Postpartum mammary gland involution drives progression of ductal carcinoma in situ through collagen and COX-2. *Nature medicine.* 2011;17(9):1109-15.

5. Miller FR, Santner SJ, Tait L, and Dawson PJ. MCF10DCIS.com xenograft model of human comedo ductal carcinoma in situ. *Journal of the National Cancer Institute.* 2000;92(14):1185-6.

6. Lyons TR, Borges VF, Betts CB, Guo Q, Kapoor P, Martinson HA, et al. Cyclooxygenase-2-dependent lymphangiogenesis promotes nodal metastasis of postpartum breast cancer. *The Journal of clinical investigation.* 2014.

7. Wallace TR, Tarullo SE, Crump LS, and Lyons TR. Studies of postpartum mammary gland involution reveal novel pro-metastatic mechanisms. *Journal of cancer metastasis and treatment.* 2019;5.

8. Borges VF, Elder AM, and Lyons TR. Deciphering Pro-Lymphangiogenic Programs during Mammary Involution and Postpartum Breast Cancer. *Front Oncol.* 2016;6:227.

9. Elder AM, Tamburini BAJ, Crump LS, Black SA, Wessells VM, Schedin PJ, et al. Semaphorin 7A Promotes Macrophage-Mediated Lymphatic Remodeling during Postpartum Mammary Gland Involution and in Breast Cancer. *Cancer research.* 2018;78(22):6473-85.

10. Fornetti J, Martinson HA, Betts CB, Lyons TR, Jindal S, Guo Q, et al. Mammary gland involution as an immunotherapeutic target for postpartum breast cancer. *J Mammary Gland Biol Neoplasia.* 2014;19(2):213-28.

11. O'Brien J, Lyons T, Monks J, Lucia MS, Wilson RS, Hines L, et al. Alternatively activated macrophages and collagen remodeling characterize the postpartum involuting mammary gland across species. *The American journal of pathology.* 2010;176(3):1241-55.

12. Gupta PB, Proia D, Cingoz O, Weremowicz J, Naber SP, Weinberg RA, et al. Systemic stromal effects of estrogen promote the growth of estrogen receptor-negative cancers. *Cancer research.* 2007;67(5):2062-71.

13. Guo Q, Minnier J, Burchard J, Chiotti K, Spellman P, and Schedin P. Physiologically activated mammary fibroblasts promote postpartum mammary cancer. *JCI Insight.* 2017;2(6):e89206.

14. Kuperwasser C, Chavarria T, Wu M, Magrane G, Gray JW, Carey L, et al. Reconstruction of functionally normal and malignant human breast tissues in mice. *Proceedings of the National Academy of Sciences of the United States of America.* 2004;101(14):4966-71.

15. McCready J, Arendt LM, Glover E, Iyer V, Briendel JL, Lyle SR, et al. Pregnancy-associated breast cancers are driven by differences in adipose stromal cells present during lactation. *Breast cancer research : BCR.* 2014;16(1):R2.

16. Asztalos S, Gann PH, Hayes MK, Nonn L, Beam CA, Dai Y, et al. Gene expression patterns in the human breast after pregnancy. *Cancer Prev Res (Phila).* 2010;3(3):301-11.

17. Black SA, Nelson AC, Gurule NJ, Futscher BW, and Lyons TR. Semaphorin 7a exerts pleiotropic effects to promote breast tumor progression. *Oncogene.* 2016;35(39):5170-8.

18. Rehman M, and Tamagnone L. Semaphorins in cancer: Biological mechanisms and therapeutic approaches. *Semin Cell Dev Biol.* 2013;24(3):179-89.

19. Tamagnone L. Emerging role of semaphorins as major regulatory signals and potential therapeutic targets in cancer. *Cancer Cell.* 2012;22(2):145-52.

20. Allegra M, Zaragkoulias A, Vorgia E, Ioannou M, Litos G, Beug H, et al. Semaphorin-7a reverses the ERF-induced inhibition of EMT in Ras-dependent mouse mammary epithelial cells. *Molecular biology of the cell.* 2012;23(19):3873-81.

21. Garcia-Areas R, Libreros S, Amat S, Keating P, Carrio R, Robinson P, et al. Semaphorin7A promotes tumor growth and exerts a pro-angiogenic effect in macrophages of mammary tumor-bearing mice. *Frontiers in physiology.* 2014;5:17.

22. Garcia-Areas R, Libreros S, Simoes M, Castro-Silva C, Gazaniga N, Amat S, et al. Suppression of tumor-derived Semaphorin 7A and genetic ablation of host-derived Semaphorin 7A impairs tumor progression in a murine model of advanced breast carcinoma. *Int J Oncol.* 2017;51(5):1395-404.

23. Ma B, Herzog EL, Lee CG, Peng X, Lee CM, Chen X, et al. Role of chitinase 3-like-1 and semaphorin 7a in pulmonary melanoma metastasis. *Cancer research.* 2015;75(3):487-96.

24. Scott GA, McClelland LA, and Fricke AF. Semaphorin 7a promotes spreading and dendricity in human melanocytes through beta1-integrins. *The Journal of investigative dermatology.* 2008;128(1):151-61.

25. Sarkar A, Barui A, Sengupta S, Chatterjee J, Ghorai S, and Mukherjee A. *2015 37th Annual International Conference of the IEEE Engineering in Medicine and Biology Society (EMBC)*. 2015:5372-5.

26. Goddard ET, Bassale S, Schedin T, Jindal S, Johnston J, Cabral E, et al. Association Between Postpartum Breast Cancer Diagnosis and Metastasis and the Clinical Features Underlying Risk. *JAMA Netw Open.* 2019;2(1):e186997.

27. Welch DRA-Ohoo, and Hurst DRA-Ohoo. Defining the Hallmarks of Metastasis. LID - 10.1158/0008-5472.CAN-19-0458 [doi]. (1538-7445 (Electronic)).

28. Cerny J, Stockinger H, and Horejsi V. Noncovalent associations of T lymphocyte surface proteins. *Eur J Immunol.* 1996;26(10):2335-43.

29. Liu H, Juo ZS, Shim AH, Focia PJ, Chen X, Garcia KC, et al. Structural basis of semaphorin-plexin recognition and viral mimicry from Sema7A and A39R complexes with PlexinC1. *Cell.* 2010;142(5):749-61.

30. Fong KP, Barry C, Tran AN, Traxler EA, Wannemacher KM, Tang HY, et al. Deciphering the human platelet sheddome. *Blood.* 2011;117(1):e15-26.

31. Jaimes Y, Gras C, Goudeva L, Buchholz S, Eiz-Vesper B, Seltsam A, et al. Semaphorin 7A inhibits platelet production from CD34+ progenitor cells. *Journal of thrombosis and haemostasis : JTH.* 2012;10(6):1100-8.

32. Xie J, and Wang H. Semaphorin 7A as a potential immune regulator and promising therapeutic target in rheumatoid arthritis. *Arthritis Res Ther.* 2017;19(1):10.

33. Kopp MA, Brommer B, Gatzemeier N, Schwab JM, and Pruss H. Spinal cord injury induces differential expression of the profibrotic semaphorin 7A in the developing and mature glial scar. *Glia.* 2010;58(14):1748-56.

34. Gan Y, Reilkoff R, Peng X, Russell T, Chen Q, Mathai SK, et al. Role of semaphorin 7a signaling in transforming growth factor beta1-induced lung fibrosis and scleroderma-related interstitial lung disease. *Arthritis and rheumatism.* 2011;63(8):2484-94.

35. Reilkoff RA, Peng H, Murray LA, Peng X, Russell T, Montgomery R, et al. Semaphorin 7a+ regulatory T cells are associated with progressive idiopathic pulmonary fibrosis and are implicated in transforming growth factor-beta1-induced pulmonary fibrosis. *American journal of respiratory and critical care medicine.* 2013;187(2):180-8.

36. Kang HR, Lee CG, Homer RJ, and Elias JA. Semaphorin 7A plays a critical role in TGF-beta1-induced pulmonary fibrosis. *The Journal of experimental medicine.* 2007;204(5):1083-93.

37. Giancotti FG. Integrin signaling: specificity and control of cell survival and cell cycle progression. *Current opinion in cell biology.* 1997;9(5):691-700.

38. Reddig PJ, and Juliano RL. Clinging to life: cell to matrix adhesion and cell survival. *Cancer Metastasis Rev.* 2005;24(3):425-39.

39. Gilmore AP, Owens TW, Foster FM, and Lindsay J. How adhesion signals reach a mitochondrial conclusion--ECM regulation of apoptosis. *Current opinion in cell biology.* 2009;21(5):654-61.

40. Hoesel B, and Schmid JA. The complexity of NF-κB signaling in inflammation and cancer. *Mol Cancer.* 2013;12:86.

41. Ozes ON, Mayo LD, Gustin JA, Pfeffer SR, Pfeffer LM, and Donner DB. NF-kappaB activation by tumour necrosis factor requires the Akt serine-threonine kinase. *Nature.* 1999;401(6748):82-5.

42. Romashkova JA, and Makarov SS. NF-kappaB is a target of AKT in anti-apoptotic PDGF signalling. *Nature.* 1999;401(6748):86-90.

43. Kane LP, Mollenauer MN, Xu Z, Turck CW, and Weiss A. Akt-dependent phosphorylation specifically regulates Cot induction of NF-kappa B-dependent transcription. *Molecular and cellular biology.* 2002;22(16):5962-74.

44. Nakao S, Ogtata Y, Shimizu E, Yamazaki M, Furuyama S, and Sugiya H. Tumor necrosis factor alpha (TNF-alpha)-induced prostaglandin E2 release is mediated by the activation of cyclooxygenase-2 (COX-2) transcription via NFkappaB in human gingival fibroblasts. *Molecular and cellular biochemistry.* 2002;238(1-2):11-8.

45. Paik J, Lee JY, and Hwang D. Signaling pathways for TNFa-induced COX-2 expression: mediation through MAP kinases and NFkB, and inhibition by certain nonsteroidal anti-inflammatory drugs. *Advances in experimental medicine and biology.* 2002;507:503-8.

46. Knowles LM, Gurski LA, Engel C, Gnarra JR, Maranchie JK, and Pilch J. Integrin αvβ3 and fibronectin upregulate Slug in cancer cells to promote clot invasion and metastasis. *Cancer research.* 2013;73(20):6175-84.

47. Lamouille S, Xu J, and Derynck R. Molecular mechanisms of epithelial-mesenchymal transition. *Nature reviews Molecular cell biology.* 2014;15(3):178-96.

48. Slocum E, Craig A, Villanueva A, and Germain D. Parity predisposes breasts to the oncogenic action of PAPP-A and activation of the collagen receptor DDR2. (1465-542X (Electronic)).

49. Guo YP, Martin Lj Fau - Hanna W, Hanna W Fau - Banerjee D, Banerjee D Fau - Miller N, Miller N Fau - Fishell E, Fishell E Fau - Khokha R, et al. Growth factors and stromal matrix proteins associated with mammographic densities. (1055-9965 (Print)).

50. Provenzano PP, Inman DR, Eliceiri KW, and Keely PJ. Matrix density-induced mechanoregulation of breast cell phenotype, signaling and gene expression through a FAK-ERK linkage. *Oncogene.* 2009;28(49):4326-43.

51. Provenzano PP, Eliceiri KW, Campbell JM, Inman DR, White JG, and Keely PJ. Collagen reorganization at the tumor-stromal interface facilitates local invasion. *BMC medicine.* 2006;4(1):38.

52. Provenzano PP, Inman DR, Eliceiri KW, Knittel JG, Yan L, Rueden CT, et al. Collagen density promotes mammary tumor initiation and progression. *BMC medicine.* 2008;6:11.

53. Kinehara Y, Nagatomo I, Koyama S, Ito D, Nojima S, Kurebayashi R, et al. Semaphorin 7A promotes EGFR-TKI resistance in EGFR mutant lung adenocarcinoma cells. *JCI Insight.* 2018;3(24).

54. Parkash J, Messina A, Langlet F, Cimino I, Loyens A, Mazur D, et al. Semaphorin7A regulates neuroglial plasticity in the adult hypothalamic median eminence. *Nature communications.* 2015;6:6385.

55. Gurrapu S, Pupo E, Franzolin G, Lanzetti L, and Tamagnone LA-Ohoo. Sema4C/PlexinB2 signaling controls breast cancer cell growth, hormonal dependence and tumorigenic potential. (1476-5403 (Electronic)).

56. Nam JM, Onodera Y, Bissell MJ, and Park CC. Breast cancer cells in three-dimensional culture display an enhanced radioresponse after coordinate targeting of integrin alpha5beta1 and fibronectin. *Cancer research.* 2010;70(13):5238-48.

57. Eke I, Storch K, Krause M, and Cordes N. Cetuximab attenuates its cytotoxic and radiosensitizing potential by inducing fibronectin biosynthesis. *Cancer research.* 2013;73(19):5869-79.

58. Murphy LC, Seekallu SV, and Watson PH. Clinical significance of estrogen receptor phosphorylation. *Endocrine-related cancer.* 2011;18(1):R1-14.

59. Pontiggia O, Sampayo R, Raffo D, Motter A, Xu R, Bissell MJ, et al. The tumor microenvironment modulates tamoxifen resistance in breast cancer: a role for soluble stromal factors and fibronectin through beta1 integrin. *Breast cancer research and treatment.* 2012;133(2):459-71.

60. Han SW, and Roman J. Fibronectin induces cell proliferation and inhibits apoptosis in human bronchial epithelial cells: pro-oncogenic effects mediated by PI3-kinase and NF-kappa B. *Oncogene.* 2006;25(31):4341-9.

61. Xiang L, Xie G, Ou J, Wei X, Pan F, and Liang H. The extra domain A of fibronectin increases VEGF-C expression in colorectal carcinoma involving the PI3K/AKT signaling pathway. *PloS one.* 2012;7(4):e35378.

62. Meng XN, Jin Y, Yu Y, Bai J, Liu GY, Zhu J, et al. Characterisation of fibronectin-mediated FAK signalling pathways in lung cancer cell migration and invasion. *British journal of cancer.* 2009;101(2):327-34.

63. Hattar R, Maller O, McDaniel S, Hansen KC, Hedman KJ, Lyons TR, et al. Tamoxifen induces pleiotrophic changes in mammary stroma resulting in extracellular matrix that suppresses transformed phenotypes. *Breast cancer research : BCR.* 2009;11(1):R5.

64. Cheng JQ, Jiang X, Fraser M, Li M, Dan HC, Sun M, et al. Role of X-linked inhibitor of apoptosis protein in chemoresistance in ovarian cancer: possible involvement of the phosphoinositide-3 kinase/Akt pathway. *Drug resistance updates : reviews and commentaries in antimicrobial and anticancer chemotherapy.* 2002;5(3-4):131-46.

65. Fraser M, Leung BM, Yan X, Dan HC, Cheng JQ, and Tsang BK. p53 is a determinant of X-linked inhibitor of apoptosis protein/Akt-mediated chemoresistance in human ovarian cancer cells. *Cancer research.* 2003;63(21):7081-8.

66. Knuefermann C, Lu Y, Liu B, Jin W, Liang K, Wu L, et al. HER2/PI-3K/Akt activation leads to a multidrug resistance in human breast adenocarcinoma cells. *Oncogene.* 2003;22(21):3205-12.

67. Li J, Feng Q, Kim JM, Schneiderman D, Liston P, Li M, et al. Human ovarian cancer and cisplatin resistance: possible role of inhibitor of apoptosis proteins. *Endocrinology.* 2001;142(1):370-80.

68. Chao Y, Wu Q, Acquafondata M, Dhir R, and Wells A. Partial mesenchymal to epithelial reverting transition in breast and prostate cancer metastases. *Cancer microenvironment : official journal of the International Cancer Microenvironment Society.* 2012;5(1):19-28.

69. Smith BN, and Bhowmick NA. Role of EMT in Metastasis and Therapy Resistance. *J Clin Med.* 2016;5(2).

70. Nurwidya F, Murakami A, Takahashi F, and Takahashi K. Molecular mechanisms contributing to resistance to tyrosine kinase-targeted therapy for non-small cell lung cancer. *Cancer biology & medicine.* 2012;9(1):18-22.

71. Nurwidya F, Takahashi F, Murakami A, and Takahashi K. Epithelial mesenchymal transition in drug resistance and metastasis of lung cancer. *Cancer research and treatment : official journal of Korean Cancer Association.* 2012;44(3):151-6.

72. Uchikado Y, Okumura H, Ishigami S, Setoyama T, Matsumoto M, Owaki T, et al. Increased Slug and decreased E-cadherin expression is related to poor prognosis in patients with gastric cancer. *Gastric cancer : official journal of the International Gastric Cancer Association and the Japanese Gastric Cancer Association.* 2011;14(1):41-9.

73. Deep G, Jain AK, Ramteke A, Ting H, Vijendra KC, Gangar SC, et al. SNAI1 is critical for the aggressiveness of prostate cancer cells with low E-cadherin. *Mol Cancer.* 2014;13:37.

74. Wang Q, Tan YX, Ren YB, Dong LW, Xie ZF, Tang L, et al. Zinc finger protein ZBTB20 expression is increased in hepatocellular carcinoma and associated with poor prognosis. *BMC cancer.* 2011;11:271.

75. Sahai E, and Marshall CJ. Differing modes of tumour cell invasion have distinct requirements for Rho/ROCK signalling and extracellular proteolysis. *Nature cell biology.* 2003;5(8):711-9.

76. McKeithen D, Graham T, Chung LW, and Odero-Marah V. Snail transcription factor regulates neuroendocrine differentiation in LNCaP prostate cancer cells. *Prostate.* 2010;70(9):982-92.

77. Cheng GZ, Chan J, Wang Q, Zhang W, Sun CD, and Wang LH. Twist transcriptionally up-regulates AKT2 in breast cancer cells leading to increased migration, invasion, and resistance to paclitaxel. *Cancer research.* 2007;67(5):1979-87.

78. Baritaki S, Yeung K, Palladino M, Berenson J, and Bonavida B. Pivotal roles of snail inhibition and RKIP induction by the proteasome inhibitor NPI-0052 in tumor cell chemoimmunosensitization. *Cancer research.* 2009;69(21):8376-85.

79. Vesuna F, Lisok A, Kimble B, Domek J, Kato Y, van der Groep P, et al. Twist contributes to hormone resistance in breast cancer by downregulating estrogen receptor-alpha. *Oncogene.* 2012;31(27):3223-34.

80. Pasterkamp RJ, Peschon JJ, Spriggs MK, and Kolodkin AL. Semaphorin 7A promotes axon outgrowth through integrins and MAPKs. *Nature.* 2003;424(6947):398-405.

81. Scott GA, McClelland LA, Fricke AF, and Fender A. Plexin C1, a receptor for semaphorin 7a, inactivates cofilin and is a potential tumor suppressor for melanoma progression. *The Journal of investigative dermatology.* 2009;129(4):954-63.

82. Jacob A, Jing J, Lee J, Schedin P, Gilbert SM, Peden AA, et al. Rab40b regulates trafficking of MMP2 and MMP9 during invadopodia formation and invasion of breast cancer cells. *Journal of cell science.* 2013;126(Pt 20):4647-58.

83. Nagy A, Lanczky A, Menyhart O, and Gyorffy B. Author Correction: Validation of miRNA prognostic power in hepatocellular carcinoma using expression data of independent datasets. *Scientific reports.* 2018;8(1):11515.

84. Barrett AS, Wither MJ, Hill RC, Dzieciatkowska M, D'Alessandro A, Reisz JA, et al. Hydroxylamine Chemical Digestion for Insoluble Extracellular Matrix Characterization. *Journal of proteome research.* 2017;16(11):4177-84.

85. Reisz JA, Nemkov T, Dzieciatkowska M, Culp-Hill R, Stefanoni D, Hill RC, et al. Methylation of protein aspartates and deamidated asparagines as a function of blood bank storage and oxidative stress in human red blood cells. *Transfusion.* 2018;58(12):2978-91.

86. Chong J, and Xia J. MetaboAnalystR: an R package for flexible and reproducible analysis of metabolomics data. *Bioinformatics.* 2018;34(24):4313-4.

87. Mi H, Muruganujan A, Ebert D, Huang X, and Thomas PD. PANTHER version 14: more genomes, a new PANTHER GO-slim and improvements in enrichment analysis tools. *Nucleic acids research.* 2019;47(D1):D419-d26.

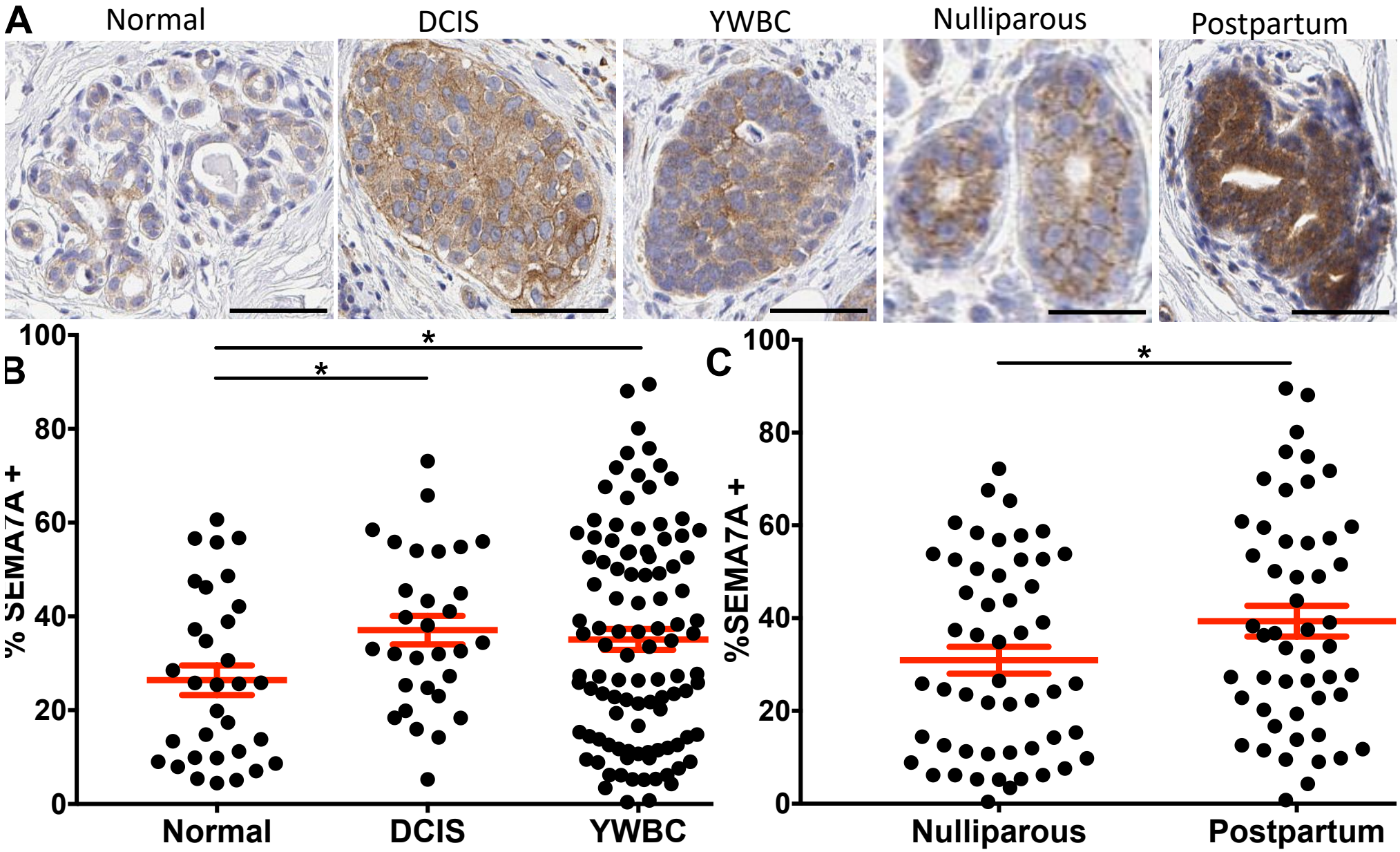
A
Normal
DCIS
YWBC
Nulliparous
Postpartum
B
% SEMA7A +
100
80
60
40
20
0
*
*
Normal
DCIS
YWBC
C
%SEMA7A +
100
80
60
40
20
0
*
Nulliparous
Postpartum

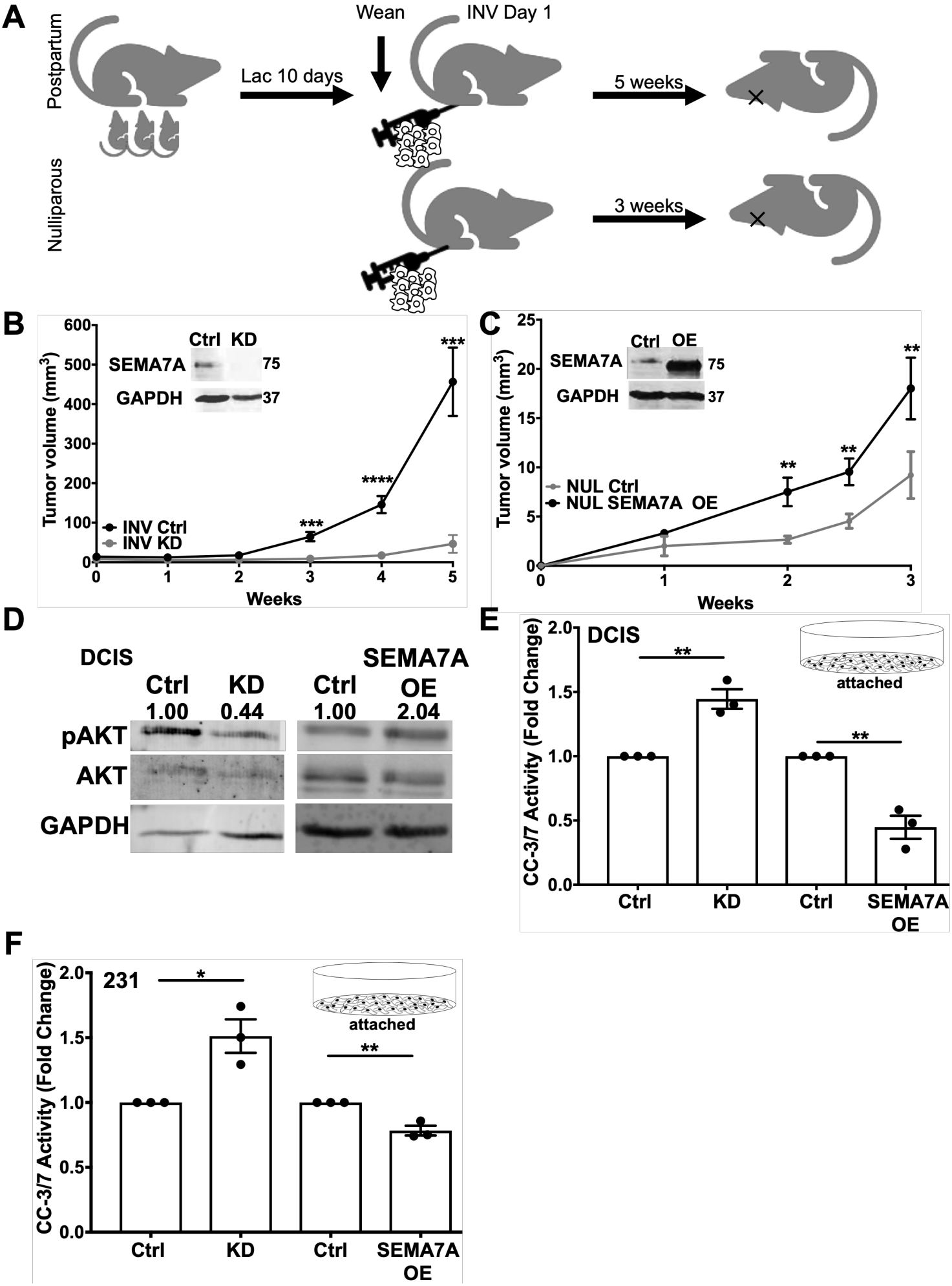
A
Postpartum
Nulliparous
Lac 10 days
Wean
INV Day 1
5 weeks
3 weeks
B
Tumor volume (mm3)
Weeks
INV Ctrl
INV KD
Ctrl KD
SEMA7A
GAPDH
75
37
***
****
***
C
Tumor volume (mm3)
Weeks
NUL Ctrl
NUL SEMA7A OE
Ctrl OE
SEMA7A
GAPDH
75
37
**
**
**
D
DCIS
SEMA7A
Ctrl KD Ctrl OE
1.00 0.44 1.00 2.04
pAKT
AKT
GAPDH
E
DCIS
attached
CC-3/7 Activity (Fold Change)
Ctrl KD Ctrl SEMA7A OE
**
**
F
231
attached
CC-3/7 Activity (Fold Change)
Ctrl KD Ctrl SEMA7A OE
*
**

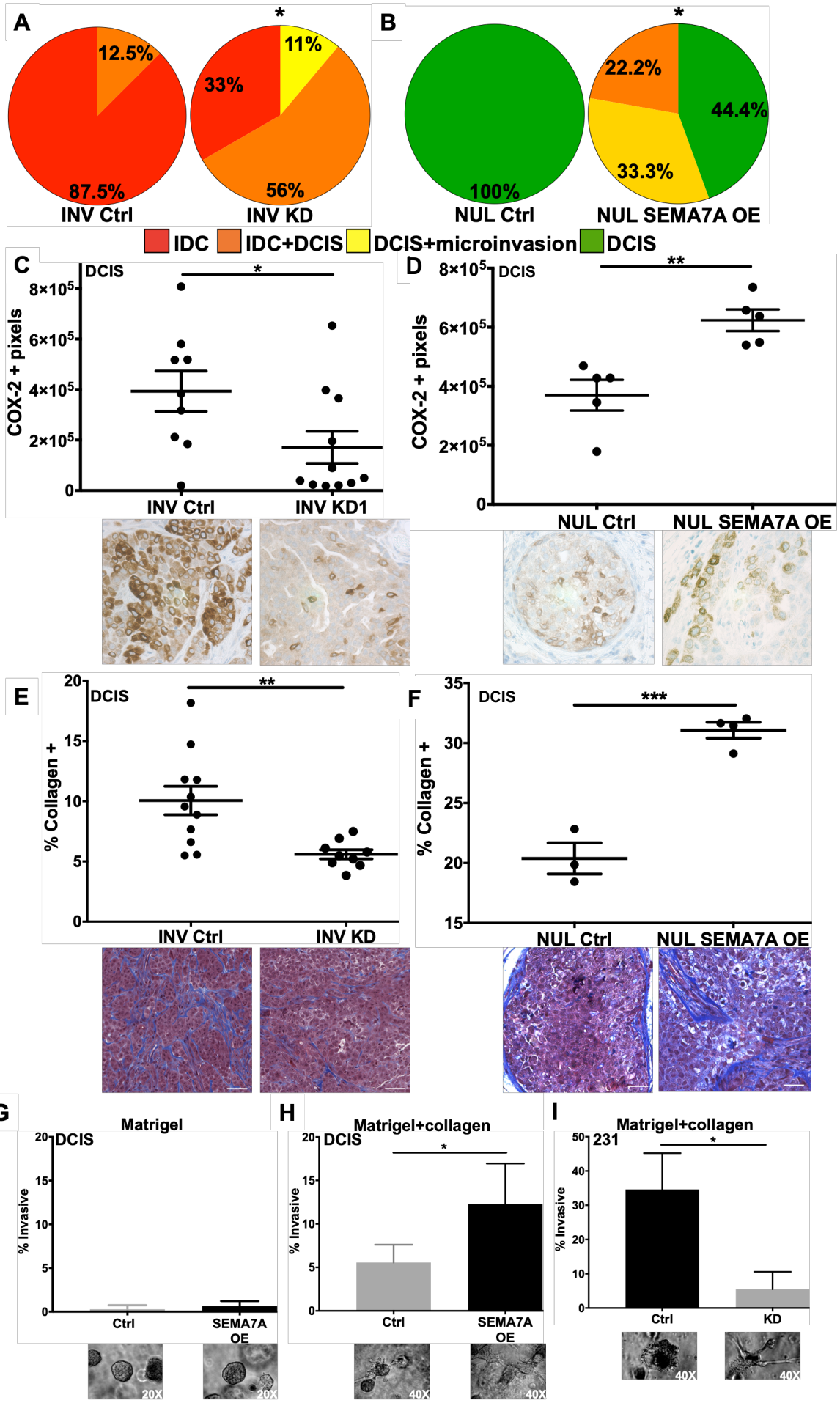
A
12.5%
87.5%
INV Ctrl
*
11%
33%
56%
INV KD
B
100%
NUL Ctrl
*
22.2%
44.4%
33.3%
NUL SEMA7A OE
IDC
IDC+DCIS
DCIS+microinvasion
DCIS
C
DCIS
*
COX-2 + pixels
8×10^5
6×10^5
4×10^5
2×10^5
0
INV Ctrl
INV KD1
D
DCIS
**
COX-2 + pixels
8×10^5
6×10^5
4×10^5
2×10^5
0
NUL Ctrl
NUL SEMA7A OE
E
DCIS
**
% Collagen +
20
15
10
5
0
INV Ctrl
INV KD
F
DCIS
***
% Collagen +
35
30
25
20
15
NUL Ctrl
NUL SEMA7A OE
G
Matrigel
DCIS
% Invasive
20
15
10
5
0
Ctrl
SEMA7A OE
20X
20X
H
Matrigel+collagen
DCIS
*
% Invasive
20
15
10
5
0
Ctrl
SEMA7A OE
40X
40X
I
Matrigel+collagen
231
*
% Invasive
50
40
30
20
10
0
Ctrl
KD
40X
40X

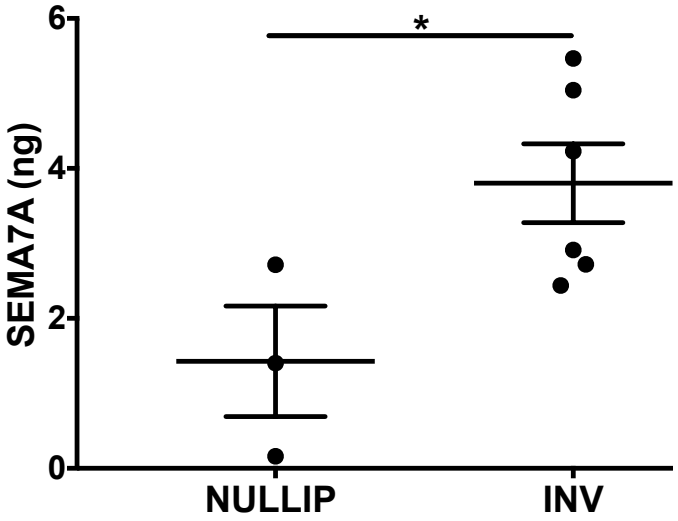
SEMA7A (ng)
6
4
2
0
*
NULLIP
INV

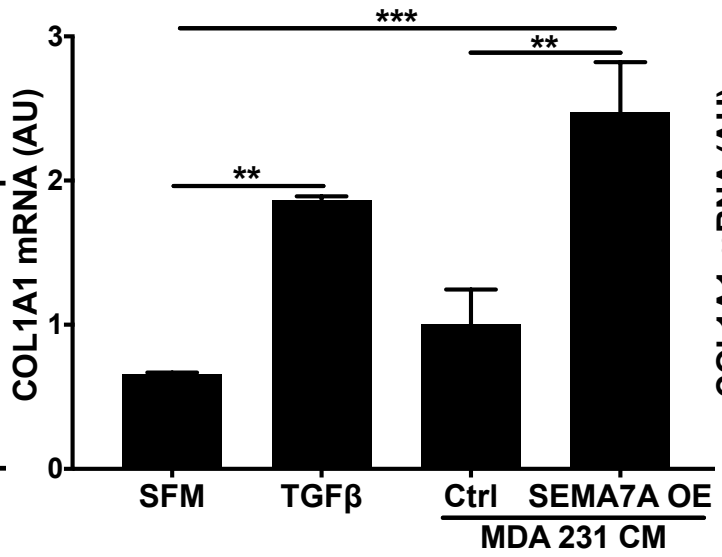
COL1A1 mRNA (AU)
3
2
1
0
***
**
**
SFM
TGFβ
Ctrl
SEMA7A OE
MDA 231 CM

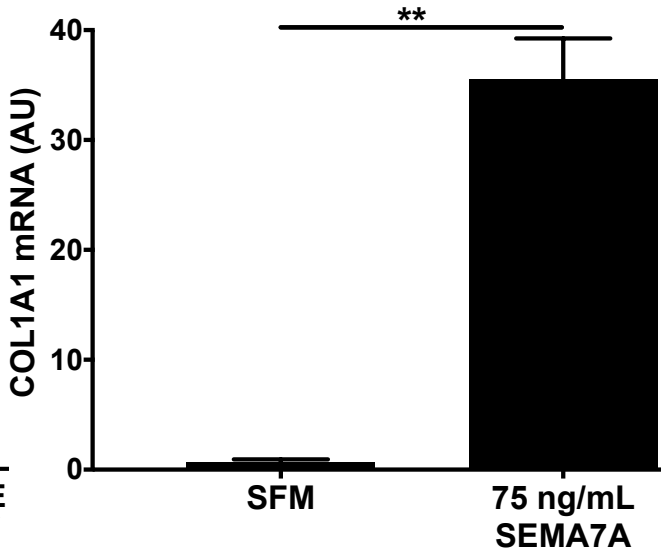
COL1A1 mRNA (AU)
40
30
20
10
0
**
SFM
75 ng/mL
SEMA7A

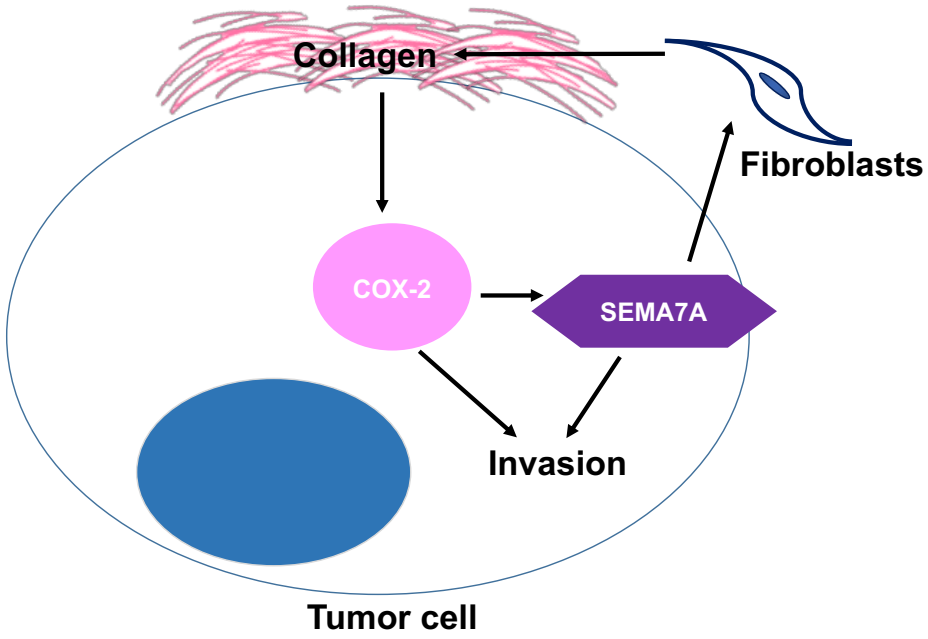
Collagen
Fibroblasts
COX-2
SEMA7A
Invasion
Tumor cell

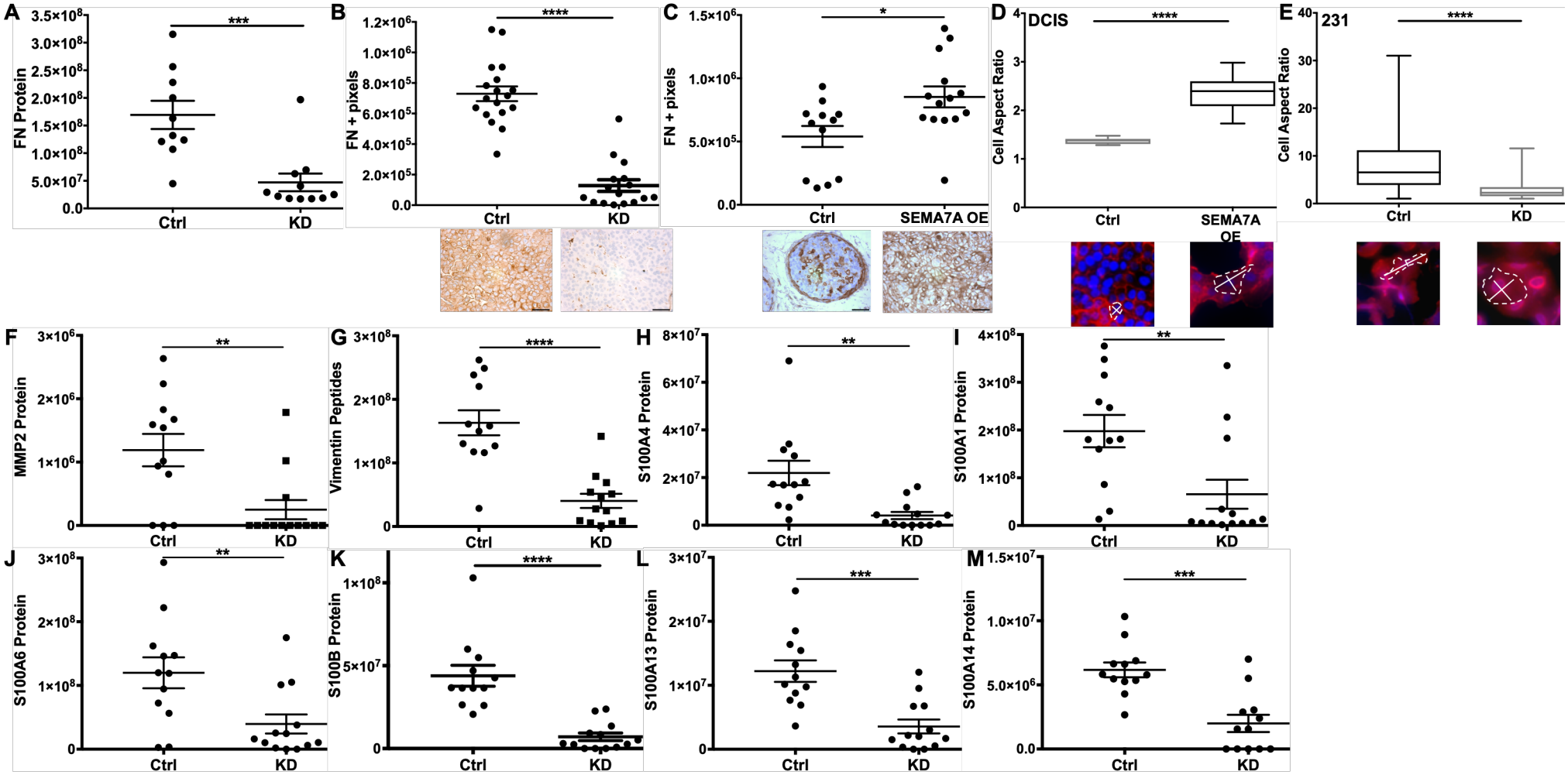
A
FN Protein
3.5×10^8
3.0×10^8
2.5×10^8
2.0×10^8
1.5×10^8
1.0×10^8
5.0×10^7
0.0
***
Ctrl
KD
B
FN + pixels
1.2×10^6
1.0×10^6
8.0×10^5
6.0×10^5
4.0×10^5
2.0×10^5
0.0
****
Ctrl
KD
C
FN + pixels
1.5×10^6
1.0×10^6
5.0×10^5
0.0
*
Ctrl
SEMA7A OE
D
DCIS
Cell Aspect Ratio
4
3
2
1
0
****
Ctrl
SEMA7A OE
E
231
Cell Aspect Ratio
40
30
20
10
0
****
Ctrl
KD
F
MMP2 Protein
3×10^6
2×10^6
1×10^6
0
**
Ctrl
KD
G
Vimentin Peptides
3×10^8
2×10^8
1×10^8
0
****
Ctrl
KD
H
S100A4 Protein
8×10^7
6×10^7
4×10^7
2×10^7
0
**
Ctrl
KD
I
S100A1 Protein
4×10^8
3×10^8
2×10^8
1×10^8
0
**
Ctrl
KD
J
S100A6 Protein
3×10^8
2×10^8
1×10^8
0
**
Ctrl
KD
K
S100B Protein
1×10^8
5×10^7
0
****
Ctrl
KD
L
S100A13 Protein
3×10^7
2×10^7
1×10^7
0
***
Ctrl
KD
M
S100A14 Protein
1.5×10^7
1.0×10^7
5.0×10^6
0.0
***
Ctrl
KD

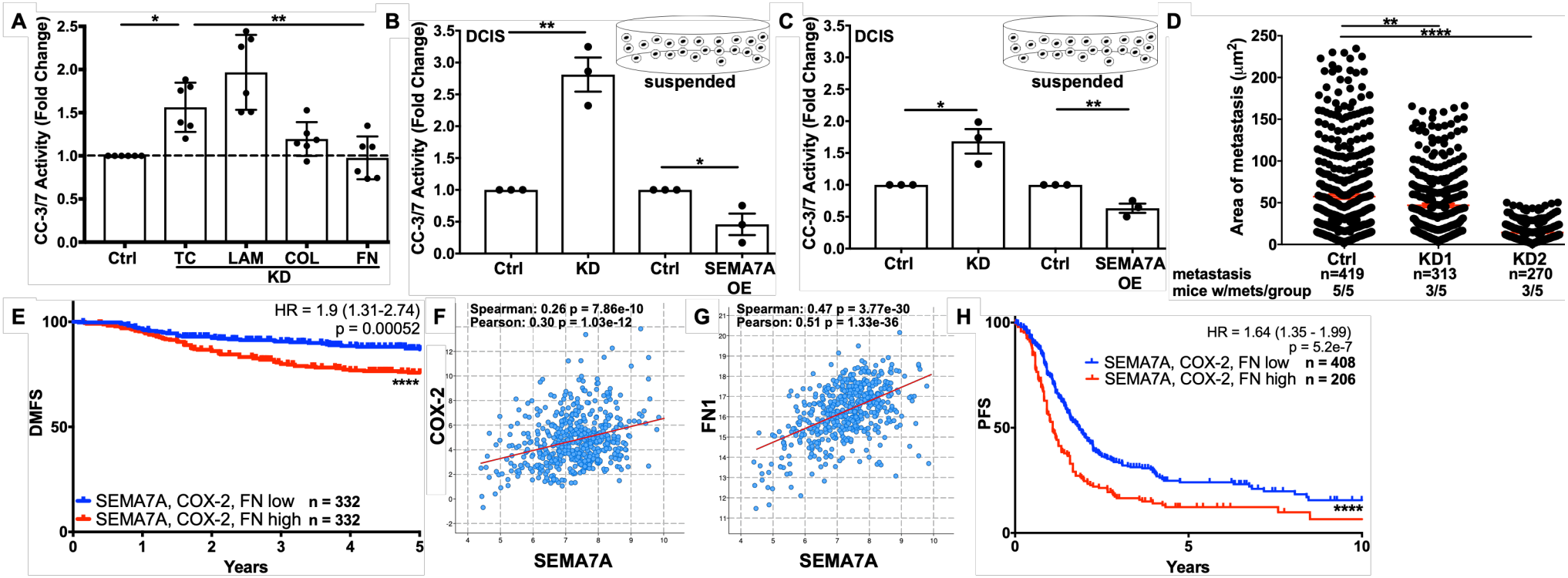
A
CC-3/7 Activity (Fold Change)
Ctrl
TC
LAM
COL
FN
KD
B
DCIS
suspended
Ctrl
KD
Ctrl
SEMA7A OE
C
DCIS
suspended
Ctrl
KD
Ctrl
SEMA7A OE
D
Area of metastasis (μm²)
Ctrl
KD1
KD2
metastasis
mice w/mets/group
n=419
5/5
n=313
3/5
n=270
3/5
E
HR = 1.9 (1.31-2.74)
p = 0.00052
DMFS
Years
SEMA7A, COX-2, FN low n = 332
SEMA7A, COX-2, FN high n = 332
F
Spearman: 0.26 p = 7.86e-10
Pearson: 0.30 p = 1.03e-12
COX-2
SEMA7A
G
Spearman: 0.47 p = 3.77e-30
Pearson: 0.51 p = 1.33e-36
FN1
SEMA7A
H
HR = 1.64 (1.35 - 1.99)
p = 5.2e-7
SEMA7A, COX-2, FN low n = 408
SEMA7A, COX-2, FN high n = 206
PFS
Years

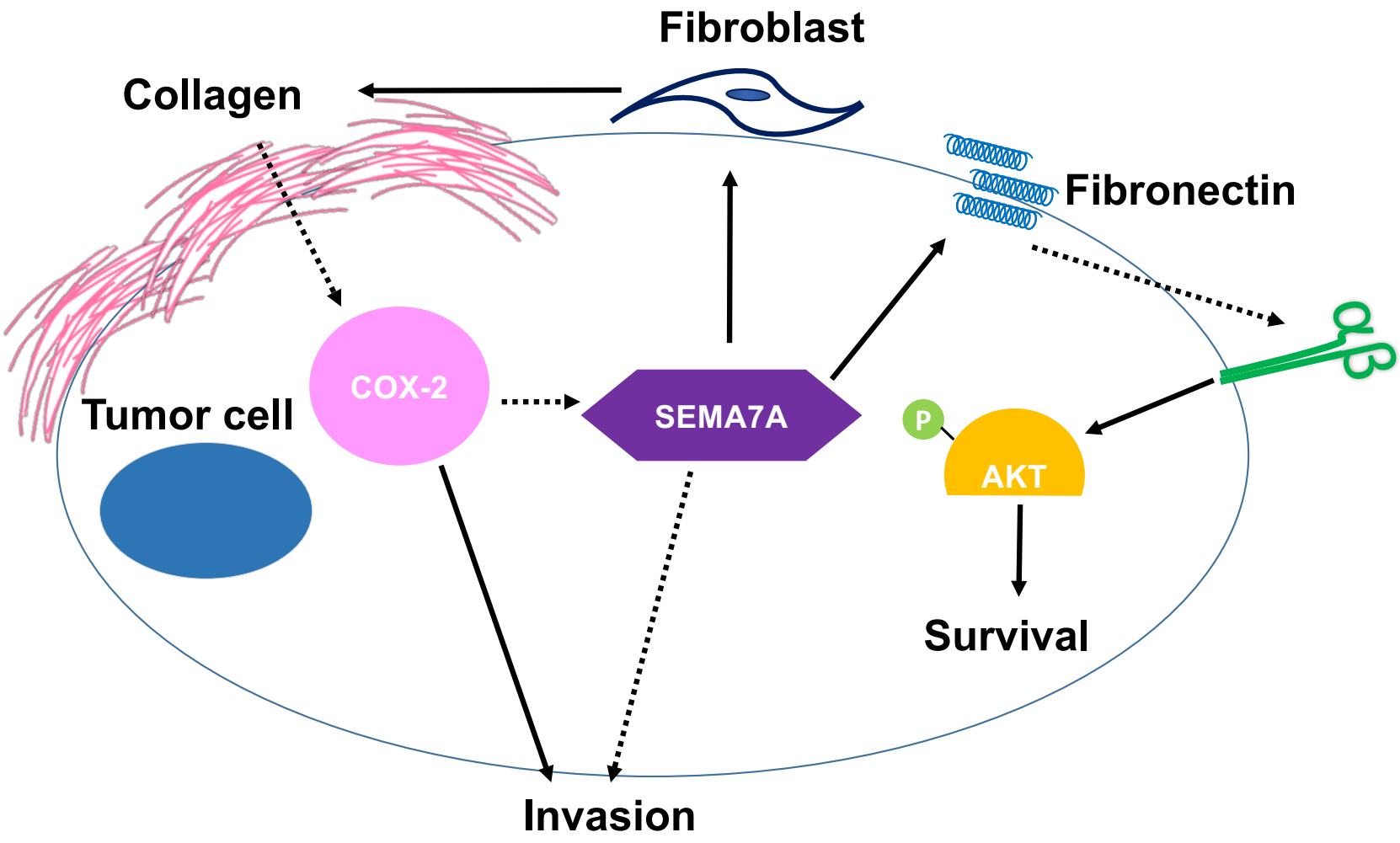
Fibroblast
Collagen
Fibronectin
αβ
COX-2
SEMA7A
Tumor cell
P
AKT
Survival
Invasion

Figure Legends

Figure 1. **SEMA7A expression in human DCIS**. **A**. Representative images of IHC for SEMA7A in normal human breast tissue, breast cancer patients with DCIS, or patients from the University of Colorado Anschutz Medical Campus Young Women's Breast Cancer (YWBC) cohort with DCIS, scale bars 50µm. **B.** Quantification of SEMA7A stain from tissue array of normal or DCIS and DCIS from YWBC cohort. (*p<0.05, t-test, two-tailed) **C**. Within the YWBC cohort, DCIS samples were separated by parody status, either nulliparous or postpartum. (*p<0.05, t-test, one-tailed).

Figure 2. **SEMA7A drives tumor growth in postpartum hosts by promoting cell survival**. **A**. Schematic of postpartum in vivo model. **B**. Tumor volumes of control (INV Ctrl) or shSEMA7A (INV KD) MCF10DCIS cells injected into postpartum hosts over five weeks, inset: immunoblot for SEMA7A and GAPDH (t-test, two tailed, ***p<0.0005, ****p<0.0001). **C**. Tumor volumes of control (NUL Ctrl) or SEMA7A overexpressing (NUL SEMA7A OE) injected into nulliparous hosts over three weeks inset: immunoblot for SEMA7A and GAPDH (t-test, two-tailed, **p<0.01). **D**. Fold change of cleaved caspase 3/7 activity in MCF10DCIS control (Ctrl), shSEMA7A (KD), or SEMA7A overexpression (SEMA7A OE) cells (t-test, two-tailed, *p<0.05, **p<0.01). **E**. Immunoblot for pAKT (S473), total AKT, or GAPDH in MCF10DCIS control (Ctrl), shSEMA7A (KD), or SEMA7A overexpression (SEMA7A OE) cell lysates. **D**. Fold change of cleaved caspase 3/7 activity in MDA231 (Ctrl), shSEMA7A (KD), or SEMA7A overexpression (SEMA7A OE) cells (t-test, two-tailed, *p<0.05, **p<0.01).

Figure 3. **SEMA7A drives invasion via collagen mediated expression of COX-2**. **A&B**. Tumors from control (INV Ctrl) or shSEMA7A (INV KD) tumors from postpartum hosts (A) or control (NUL Ctrl) or SEMA7A overexpressing (NUL SEMA7A OE) tumors from nulliparous hosts (B) scored for invasion (*p<0.05, t-test, two-tailed). **C&D**. IHC quantification (top) and representative images (bottom) of IHC for COX-2 of tumors from control (INV Ctrl) or shSEMA7A (INV KD) tumors from postpartum hosts (C) or control (NUL Ctrl) or SEMA7A overexpressing (NUL SEMA7A OE) tumors from nulliparous hosts (D) (*p<0.05, **p<0.01, t-test, two tailed). **E&F**. Trichrome stained quantification (top) and representative images (bottom) of COX-2 of tumors from control (INV Ctrl) or shSEMA7A (INV KD) tumors from postpartum hosts (E) or control (NUL Ctrl) or SEMA7A overexpressing (NUL SEMA7A OE) tumors (F) from nulliparous hosts (*p<0.05, ***p<0.005, t-test, two tailed). **G**. Ctrl or SEMA7A OE MCF10DCIS cells embedded in 3D culture consisting of only matrigel sored for invasion. **H**. Ctrl or SEMA7A OE MCF10DCIS cells embedded in 3D culture of matrigel with the addition of 20% collagen reveals an increase in percent of invasive organoids (*p<0.05, t-test, two tailed). **I**. Ctrl or shSEMA7A (KD) MDA 231 cells in 3D culture scored for invasion (*p<0.05, t-test, two tailed).

Figure 4. **Shed SEMA7A promotes fibroblast collagen deposition**. **A**. Shed SEMA7A levels from conditioned media harvested from tumor cells lines derived from nulliparous (NULLIP) or postpartum (INV) hosts, measured via ELISA. **B**. Quantitative RT-PCR (q-PCR) for *COL1A1* in fibroblasts in serum free media (SFM) treated with 10 ng/mL TGFβ or conditioned media (CM) from control (Ctrl) or SEMA7A overexpressing (SEMA7A OE) MDA 231 cell lines. **C**. qPCR for *COLA1A* in fibroblasts in SFM treated with 75 ng/µL of purified SEMA7A. **D**. Interim summary depicting the interplay between, SEMA7A, COX-2, fibroblasts, and collagen in mediating tumor cell invasion.

Figure 5. **SEMA7A drives fibronectin expression and mesenchymal phenotypes**. **A**. Global proteomics analysis reveals a decrease in fibronectin (FN) expression in MCF10DCIS shSEMA7A (KD) tumors compared to control (Ctrl) ex vivo (***p<0.001, t-test, two-tailed). **B&C**. IHC for FN in MCF10DCIS Ctrl and KD tumors (B), and MCF10DCIS Ctrl and SEMA7A overexpressing (SEMA7A OE) tumors, scale bar 50µm (****p<0.001, *p<0.05, t-test, two-tailed). **D**. Immunofluorescence for F-actin in MCF10DCIS Ctrl or SEMA7A OE cells, quantified for cell aspect ratio (length/width) (****p<0.001). **E**. Immunofluorescence for F-actin in MDA 231 Ctrl or KD cells, quantified for cell

aspect ratio (length/width) (****p<0.001). **F-M**. Global proteomics analysis reveals several mesenchymal or mesenchymal associated proteins are decreased in shSEMA7A (KD) tumors ex vivo.

Figure 6. **SEMA7A drives metastatic progression and poor prognosis**. **A**. Fold change of cleaved caspase 3/7 activity control (Ctrl) or shSEMA7A (KD) cells plated on tissue culture plastic (TC), laminin (LAM), collagen I (COL) or fibronectin (FN) (ANOVA, *p<0.05, **p<0.01). **B&C**. Fold change of cleaved caspase 3/7 activity MCF10DCIS (F) or MDA231 (G) control (Ctrl), shSEMA7A (KD), or SEMA7A overexpression (SEMA7A OE) cells in forced suspension (t-test, two-tailed, *p<0.05, **p<0.01). **D**. Average area of metastasis formed in lungs of mice injected via the tail vein with MDA 231 control (Ctrl) or shSEMA7A (KD1, KD2) cells (ANOVA, **p<0.01, ****p<0.001). **E**. Kaplan-Meier analysis of breast cancer using Km plotter for SEMA7A, COX-2 and FN mRNA expression for distant metastasis free survival (DMFS) (****p<0.001). **F&G**. Co-expression analysis of the TCGA breast cancer provisional cohort using CbioPortal reveals significant correlations between SEMA7A and COX-2 (F) and SEMA7A FN (G) expression. **H**. Kaplan-Meier analysis of ovarian using Km plotter for SEMA7A, COX-2 and FN mRNA expression for progression free survival (DMFS) (****p<0.001).

Figure 7. **Model depicting SEMA7A mediated invasion and cell survival.** Previously we have shown collagen mediated COX-2 expression results in tumor cell survival. Our current data suggests SEMA7A promotes fibroblast mediated collagen deposition, resulting in COX-2 expression and invasion. SEMA7A can also play a role in promoting cell survival; this may be through SEMA7A-β1 integrin signaling or through SEMA7A mediated fibronectin expression.